

# Delayed Baroclinic Response of Antarctic Circumpolar Current to Surface Windstress

Xiao -Yi Yang<sup>1</sup> Ruixin Huang<sup>2</sup> Jia Wang<sup>3</sup> Dongxiao Wang<sup>1</sup>

(1. South China Sea Institute of Oceanology, Chinese Academy of Sciences, Guangzhou 510301 ; 2.

Woods Hole Oceanographic Institution , MA02543 USA ; 3. NOAA Great Lakes Environmental

Research Laboratory (GLERL), Michigan 48105 USA.

E-mail: dxwang@scsio.ac.cn)

**Abstract** Antarctic Circumpolar Current (ACC) responds to the surface windstress via two processes, i.e., instant barotropic process and delayed baroclinic process. This study focuses on the baroclinic instability mechanism in ACC. That is, the strengthening of surface zonal windstress causes the enhanced tilting of the isopycnal surface, which leads to the intense baroclinic instability. Simultaneously, the mesoscale eddies resulting from the baroclinic instability facilitate the transformation of mean potential energy to eddy energy, which causes the remarkable decrease of the ACC volume transport with the 2-year lag time. This delayed negative correlation between the ACC transport and the zonal windstress may account for the steadiness of the ACC transport in these two decades.

**Key words:** Antarctic Circumpolar Current (ACC); zonal windstress; baroclinic instability; mesoscale eddy.

The Antarctic Circumpolar Current may be the most powerful flow among the global oceans, with its transport of about 130-140Sv ( $1\text{Sv}=10^6\text{m}^3/\text{s}$ ). ACC connects and transfers heat, salt and other materials between the three global ocean basins, and plays an important role in global climate change<sup>[1]</sup>. The ACC momentum balance has its own distinct features, which made it a hot topic for a long time. But no consensus has been reached so far.

It is well known that the zonal transport of ACC is mainly driven by the surface windstress. From the dynamical viewpoint, this driving mechanism can be realized via two processes: one is the rapid barotropic response process, involving the direct zonal momentum transport from the windstress to the ACC; another is, in contrast, the slow baroclinic process, that is, surface windstress changes the ocean density stratification and further influences the ACC transport indirectly. Webb and Cuevas<sup>[2]</sup> simulated the rapid response of the Southern Ocean to the zonal windstress, and found that the ACC transport responded to windstress in about two days via a topography-oriented barotropic process. Another numerical model study also demonstrated that the maxima of Drake Passage transport appeared in lagging the surface westerly maxima for 3 days<sup>[3]</sup>. On the other hand, the positive (negative) anomalies of the surface windstress causes not only the acceleration (deceleration) of the ACC but also the weakening (strengthening) of the subsurface stress and bottom pressure<sup>[4, 5]</sup>. This transport variability exhibits the feature of barotropy along potential vorticity isolines in the intraseasonal time scale<sup>[6]</sup>. Meridith et al.<sup>[7]</sup> suggested that the interannual variability of Drake Passage transport was related to the surface windstress, which presented the strong baroclinicity independent of sea surface height. Another support for this conclusion is from Hughes and Stepanov<sup>[8]</sup>, who showed no significant correlation between the interannual variability of the ACC transport and the surface windstress in a barotropic model. This indicates that in addition to the direct momentum input, the windstress can change the ACC stratification via Ekman pumping. Ekman pumping, along with the buoyancy forcing (e.g., cooling in the south and heating in the north), produces a baroclinic pressure gradient, leading to the vertical shear of ACC zonal velocity and baroclinic transport<sup>[9]</sup>. Gnanadesikan and Hallberg<sup>[10]</sup> used a low resolution ocean model to simulation the impact of the Southern Ocean surface wind to circumpolar current. Their results indicate that the enhancing westerly favors the increase of the northward Ekman transport, the deepening of pycnocline and the warming of the deep water in the north of Southern Ocean. The resulting enhancement of the vertical shear leads to the strengthening of the ACC baroclinic transport. It should be noted that this result may be inaccurate as the low resolution ocean model can not resolve the mesoscale eddies.

Mesoscale eddies play an important role in the ACC momentum balance. The Drake Passage latitude ocean is zonally unbounded, thus the momentum input by surface windstress can be balanced neither by the zonally pressure gradient nor the lateral Reynolds stress. To balance the momentum

input and the excessive acceleration of ACC, the mesoscale eddies have to transport the surface momentum to the deeper level. In addition, the mesoscale eddies induce the disturbances in the tilting isopycnals and zonal pressure gradient, which, via interfacial form stress, further transport the horizontal momentum across the isopycnals. In this sense, the mesoscale eddies may be a key factor to determine the Southern Ocean stratification and the zonal transport<sup>[11, 12]</sup>.

The current research results may partly describe the ACC zonal momentum balance as following: The momentum input of the eastward windstress is transport downward to the ocean deeper level by the effect of standing and transient eddies. The form stress comes from the bottom pressure field, which, plus the bottom friction force, comprises of the sink of the zonal momentum and balances the surface windstress. Hence, surface windstress and mesoscale eddy activity are the two important dynamical factors to influence the variability of the ACC transport.

This study focuses on the connection between the ACC transport and the zonal windstress. We found that the two factors exhibit no consistent linear trends in the decadal time scales, although their interannual correlation is significant. That is, the windstress presented a strong upward trend during 1980-1999, whereas the ACC transport remained relatively steady. Our results suggest this inconsistency may be attributed to the mesoscale eddy activity in the Southern Ocean: in addition to drive the zonal mean flow, windstress tends to tilt the isopycnals; the resulting increase of the horizontal density gradient begets the strong baroclinic instability, which facilitates the transformation of mean flow energy to eddy energy; the strengthening of mesoscale eddy activity transport the surface momentum input downward to the deep ocean, and deplete the momentum through bottom form stress; thus the ACC transport could maintain its steadiness in the recent two decades.

## **1 Data and method**

Simple Ocean Data Assimilation (hereafter SODA) reanalysis dataset is used to do statistical analysis in this study. SODA is a set of ocean assimilation data, which simultaneously assimilates the in-situ observations and satellite measurements on the basis of a global ocean circulation model (GFDL MOM2.2), including temperature, salinity and flow velocities<sup>[13]</sup>. The time span is 1958-2001 monthly mean data. The spatial resolutions are  $0.25^{\circ} \times 0.4^{\circ}$  (projecting on the  $0.5^{\circ} \times 0.5^{\circ}$  grid) in the horizontal and 40 levels in the vertical, ranging from surface 5m to 5347m. The model is forced by the ECWMF

40-year (ERA40) reanalysis daily surface wind field. This SODA dataset is more reliable than other model output data for its assimilation of in-situ data and more consistent and complete temporally and spatially in comparison with the in-situ data.

Isopycnal slope can be calculated from  $S = -\frac{|\nabla_h \sigma|}{\sigma_z}$ , i.e., the ratio of the horizontal gradient with

vertical gradient of potential density. The baroclinic conversion rate of the ACC comes from the baroclinic conversion term in the perturbation energy equation (see appendix for the detailed formula). The baroclinic conversion rate could denote the extent of the conversion of mean flow potential energy to the eddy energy via baroclinic instability process. The value of the baroclinic conversion rate is controlled by the two factors: one is the vertical component of EP flux (which denotes the strength of eddy activity), and the other is the mean flow stratification (which denotes the baroclinic instability of the background field).

## 2 Response of the ACC to the surface windstress

Previous studies showed that the primary variability mode of the Southern Hemisphere (SH) zonal windstress exhibits a zonally symmetric equivalent barotropic structure, i.e., the north-south vacillation dipole mode between 40°S and 60°S. This mode can explain the 33%<sup>[14]</sup> and 30%<sup>[15]</sup> of total variance in the ten-day low-pass data and monthly mean data, respectively. However, some scientists indicated that the SH atmospheric circulation had remarkable interdecadal variability other than the interannual variability. This interdecadal variability can be displayed on the Southern Annular Mode (SAM) and the westerly jet<sup>[16, 17]</sup>. Furthermore, the zonal windstress showed a significant upward trend during 1980-1999<sup>[18, 19, 20]</sup>. To clearly depict the influence of this decadal variability of zonal wind stress to the ACC, we drew the spatial map of the surface windstress linear trends overlapped by the ACC stream function climatology (Fig. 1). It was clear that the ACC lay between the 65°-45°S latitudinal belt with the quasi-zonal structure. Interestingly, the zonal windstress also exhibited a linear

strengthening trend with zonally symmetric mode, and its positive maxima are superposed with the axis of the ACC.

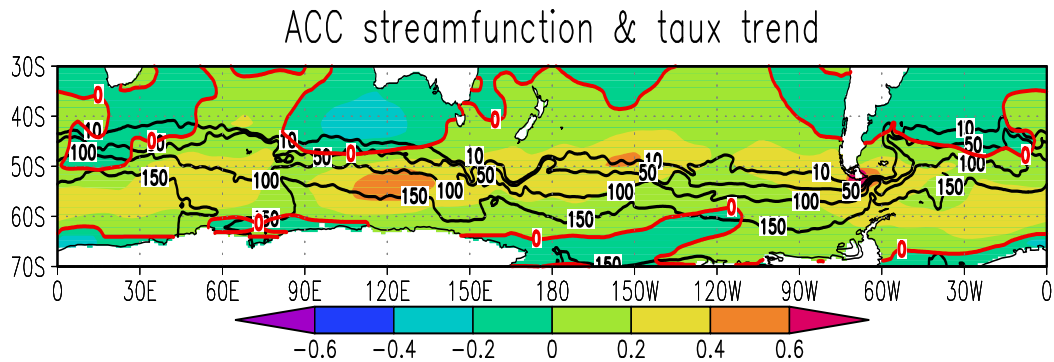


**Fig. 1.** 1980-1999yr ACC steam function climatology (black contours, unit: Sv) and zonal windstress linear trend (shaded, unit: dyn/cm/20yr). The red contours denote the zero lines of wind stress trend.

In virtue of the zonal symmetric feature of the ACC and the surface windstress, we calculated the area average windstress between the 65°-45°S belt, and then compared its time series (Fig. 2a) with the time series of the Drake Passage transport (Fig. 2b). Obviously, there are 4-5 yr period for both time series, and their interannual correlation can be 0.419, up to the 95% significance level. Thus on the interannual time scale, the strengthening of the windstress is related to the increase of the ACC transport.

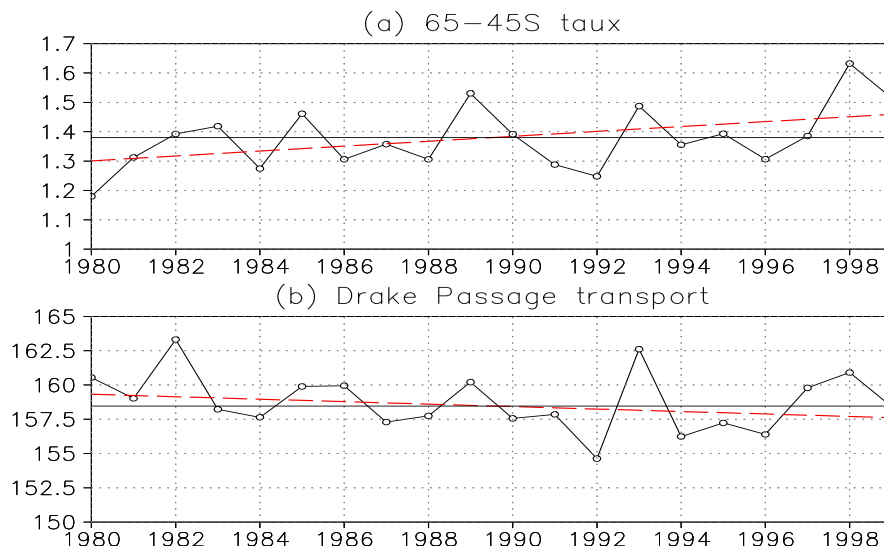


**Fig. 2.** Time series of the 65°-45°S area averaged (a) windstress (unit:  $\text{dyn}/\text{m}^2$ ); (b) Drake Passage transport (unit: Sv) and their linear trends (dashed lines). The correlation coefficient for the two time series is 0.419; and their lag 2 yr correlation is -0.589; Both are significant for the 95% t-test.

We then analyzed the linear trend terms: for windstress, the linear trend is  $0.167$  ( $\text{dyn}/\text{cm}^2/20\text{yr}$ ), which is much larger than its standard deviation ( $\pm 0.106$   $\text{dyn}/\text{cm}^2$ ). In another word, the windstress exhibited a remarkable strengthening tendency in the recent two decades. However, we should note that the significant correlation between the windstress and the ACC can only emerge on the interannual time scale, but not on the decadal time scale. In spite of the continuous strengthening of the surface windstress, the ACC transport remained relative steadiness for the decadal time scale as its linear trend ( $-1.797\text{Sv}/20\text{yr}$ ) was not significant compared with its standard deviation ( $\pm 2.095\text{Sv}$ ). It's well-known that surface windstress is the main driven of the ACC, and also on the interannual time scale, they two displayed a rather high positive correlation. But why were they inconsistent on the decadal time scale? In the next section, we try to answer this question by using the ACC momentum balance analysis and the baroclinic instability mechanism

### **3 The mesoscale eddy activity and its role in the ACC momentum balance**

Here we try to explore the process of windstress momentum input, its downward propagation and the balance between the windstress momentum and the bottom form stress. Recent studies showed that the downward propagation of horizontal momentum could be realized by the mesoscale eddies (with the horizontal scale of about 150km) and the topographic standing waves. Hallberg and Gnanadesikan<sup>[21]</sup> proposed the “eddy saturation” effect, that is, the ACC transport manifests a linear correlation with the windstress forcing at the stage of weak wind or buoyancy-dominating (diabatic process), while in the strong wind case, it is the eddy field that varies with the windstress; In the latter case, the ACC transport remained steady. Meredith and Hogg<sup>[22]</sup> found that the eddy kinetic energy (EKE) maxima always lagged to the surface windstress maxima by about 2-3 years in the satellite data. Using an eddy-resolving model, they suggested that this lagging effect may largely due to the baroclinic adjustment process, i.e., the wind energy input is first stored as the mean flow potential energy; then the mesoscale eddies, by the form stress effect, transfer the momentum from upper layer

to topographic deep ocean; the topographic effect further enhances the baroclinic instability of the mean flow, facilitating the conversion of mean potential energy to the eddy energy (either eddy potential energy or eddy kinetic energy); then the windstress momentum input can be dissipated gradually by eddy effect.

In our statistical analysis results, the interannual correlation between the zonal windstress and ACC transport existed not only simultaneously, but also for lagging period. The lag 2yr correlation can be -0.589, which is far above the 95% significance level. Hereby we suggested that the strengthening of ACC transport in response to the windstress intensification was followed by the lag 2-yr weakening of ACC transport, which was probably connected with the ACC baroclinic instability and relevant eddy activity.

To testify this speculation, we calculated the Southern Ocean isopycnal slope as it can be used to roughly denote the ocean stratification stability against baroclinic perturbation. More tilting is isopycnal layer, the stratification tends more baroclinic instability. 60°-45°S area-mean isopycnal slopes for the ACC upper ocean (25m and 268m) were showed in Fig. 3.

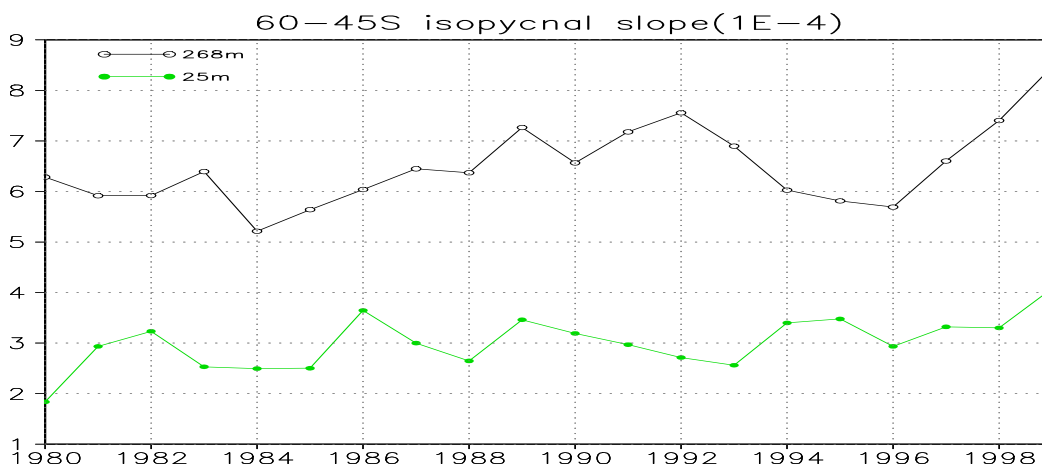


**Fig. 3.** Time series of 60°-45°S area-mean isopycnal slope. The line with open circle denotes the 269m level slopes, while that with solid circle is 25m level slopes. The two time series both exhibited an upward trend, i.e., the isopycnal slopes tilted more and more intense.

The isopycnal slopes showed an upward trend during 1980-1999, while before 1980, the trend was unobvious. This may closely relate to the surface windstress acceleration: due to the effect of geostrophy, the zonal wind acceleration lead to the continuous strengthening of northward Ekman

transport in upper ocean, which, along with the anomalies of vertical velocity (ascending in the south and descending in the north), drives the acceleration of the local meridional circulation. The subsequent tilting of the isopycnal slope corresponds to the increase of mean flow potential energy, then the ACC is apt to be baroclinic instability. The mesoscale eddies released by the unstable mean flow undoubtedly influence the ACC momentum balance. In the ACC region, the baroclinic instability will induce the energy transfer from the large-scale to the meso-scale. This part of energy is basically balanced with the windstress energy input to ocean. Eddy activity could produce the poleward heat flux (balancing the air-sea heat flux) as well as the downward propagation of the eastward momentum flux (balancing the surface wind momentum input). In this sense, the eddy-induced downward propagation of momentum may be regarded as the key factor to the ACC momentum balance<sup>[23]</sup>. We further explore the effect of mesoscale eddies in the ACC momentum balance, by using EP flux and baroclinic conversion rate calculation.

EP flux section (figure not shown) revealed that the vertical propagation direction of eddy perturbation was consistently downward, extending to the upper 2km ocean. The vertical component of EP flux (i.e., the ratio of the eddy density flux to the stratification) may be used to denote the form stress effect in the ACC region, that is, the surface momentum is transferred by the eddies (through the form stress effect) downward to the deep ocean, and then balanced by the topographic form stress.

From the above analysis, the decadal strengthening of the zonal windstress corresponds to the stronger tilting of isopycnal slope and the mean flow baroclinic instability. To further explore the connection of baroclinic instability and zonal windstress, we calculated the baroclinic conversion rate (formula in the appendix), and plot the lag composite map of 60-45°S averaged baroclinic conversion rate for the zonal windstress high index (above one standard deviation) (Fig. 4).

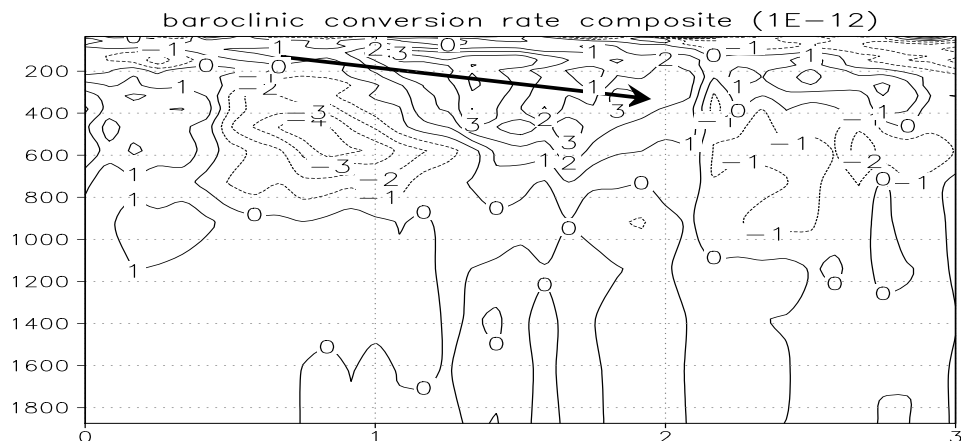




Fig. 4. Composite map of the 60-45°S averaged baroclinic conversion rate (unit:  $\text{m}^2/\text{s}^3$ ); the x-axis denotes the lagging year of conversion rate to windstress, while y-axis is the depth (unit: m). Black vector illustrates the positive anomaly centers of baroclinic conversion rate in different time lag stage. The positive anomaly (corresponding to the conversion of mean flow potential energy to eddy energy) appears firstly in the half-year lag period at the upper ocean (above 200m); this anomaly seems to propagate downward with time, and reaches to the 1km level in the 2yr lag; and diminishes hereafter.

It was clear that the baroclinic conversion rate presented the negative anomalies at the zero lag, (keep in mind that the baroclinic conversion rate climatology is unanimously positive in the whole ACC region, figures not shown, indicating the energy conversion from mean flow to eddies), thus the energy conversion from the mean flow to eddies decreased. This increased the mean flow potential energy, and then necessitates the enhancement of ACC baroclinic transport according to ocean thermal wind relation. The negative anomaly propagated downward to deeper ocean (about 1km) at the half-year lag, which may partly account for the positive correlation between the ACC transport and zonal windstress. More importantly, along with the downward propagation of negative anomaly, the positive anomaly of conversion rate appeared at the ocean surface. This positive anomaly also propagated downward to 1km depth at the one and a half year or two-year lag, and then weakened after two years. Since the positive anomaly of conversion rate denoted the intensification of ACC mean potential energy to eddy energy, the windstress acceleration may induce the positive anomaly of baroclinic conversion, facilitating the energy conversion from mean flow to eddy, hereby dissipating the mean flow energy and diminishing the ACC transport.

#### **4 Conclusion and discussion**

Many model studies simulated the consistent upward trend of surface windstress and the ACC transport in the decadal time scale, but we noted that these models were always low-resolution without the sufficient response of mesoscale eddies to the windstress, and the role of eddies in the ACC

momentum balance was underestimated. Some recent in-situ data analysis (ISOS and WOCE data) did not support the significant decadal trend of the ACC transport, which is consistent with our results. According to our analysis, the significant interannual correlation existed between the ACC transport and surface wind. The ACC will accelerate instantly in response to the windstress increase. However, the ACC dropped down after two years. This lagging negative correlation connected closely with the ACC baroclinic instability mechanism: zonal windstress drove the northward Ekman transport in the geostrophic effect, which induced the acceleration of the local wind-driven meridional circulation and the stronger tilting of isopycnal slope; the resulting baroclinic instability activated the mesoscale eddies, and transformed the mean potential energy to eddy energy, leading to the 2-yr lag deceleration of the ACC transport. It was this baroclinic dissipation effect of mesoscale eddies that kept the ACC transport from the impact of surface windstress, and maintained its steadiness during the recent two decades. It was deserved noting that windstress and the ACC transport both presented 4-5 period in the interannual time scale, which bore great comparability with the interannual variability of tropical air-sea interaction phenomenon (ENSO). Zhou and Yu<sup>[25]</sup> found that the Southern Annular Mode (SAM) was influenced by the El Nino, and this effect had rather high predictability. In this sense, there may be certain connection between the high-latitude air-sea interaction and tropical air-sea interaction. Further study of the interannual variability of ACC needs to include the effect of both mid-latitude atmosphere and tropical oceans.

As the SODA data is a monthly data and its spatial resolution is only  $0.5^{\circ} \times 0.5^{\circ}$ , the eddy flux and baroclinic conversion rate calculated in this study may be attributed mainly to the topographic-oriented standing eddies. In contrast, the large portion contribution from the transient eddies was not included. But previous study showed that the small scale standing eddies (the curve and distortion in the sharp topographic region of the ACC axis) could be regarded as the mesoscale eddies; eddies became dominate when the windstress enhanced, and the baroclinic instability always emerged in the rough topographic regions through the effect of standing waves. Therefore, the connection of ACC transport and windstress relied on the response process of the standing eddies<sup>[21]</sup>. The model study of Wang and Ikeda<sup>[26]</sup> demonstrated the influence of the bottom topography to the growth rate of the baroclinic instability wave. Thus the mesoscale eddy activity and its effect on the mean flow should depend on topography. In addition, we used Estimating the Circulation and Climate of the Ocean (ECCO-JPL)

dataset with resolutions of 10-day temporally and  $1^\circ \times 1^\circ$  spatially to calculate the baroclinic conversion rate. The analysis results are basically consistent with this study. Due to the relative high temporal resolution of ECCO data, it should depict the transient eddy activity more accurately. This justified our results to some extent. On the other hand, the standing eddies and transient eddies both will respond to the windstress variability in the stage of strong wind, and both acted as the brake to the zonal mean flow to balance the wind energy input. Therefore, in order to accurately depict the Southern Ocean large-scale circulation variability and momentum balance, we need higher (eddy-resolving) resolution dataset to study the eddy activity and eddy flux in the Southern Ocean.

## Appendix

Since the ACC is zonally unbounded, its dynamics bears much similarity with the atmospheric dynamics. In this study, EP flux and oceanic wave-mean flow interaction methods were used to explore the ACC momentum balance.

Eliassen-Palm theory was first put forward by Eliassen and Palm<sup>[28]</sup>. According to this theory, the effect of the wave perturbation to zonal mean flow is diagnosed from the vector  $F$  (EP flux) in the meridional section. The EP flux satisfies the quasi-geostrophic approximation in the  $\beta$  plane and its two components denote the poleward eddy heat flux and eddy momentum flux respectively. In the Southern Ocean, the fresh water flux due to the sea ice melting may impose on the ocean density stratification.

Thus we generalized the EP flux as the form of  $F = -\overline{u'v'\hat{y}} + \frac{f}{\rho_z} \overline{v'\rho'z}$ ; the first term in the right

hand side is eddy momentum flux, denoting the horizontal propagation of wave perturbation, while the second term is the ratio of eddy density flux and mean stratification, denoting the vertical propagation of perturbation.

EP flux is always used to diagnose the wave-mean flow interaction. According to the EP theory and energy conservation theory, perturbation energy equation can be written as

$$\partial_t \iiint (K' + A') = -\partial_t \iiint (K_m + A_m) = -\iiint U \nabla \square F .$$

Obviously, EP flux divergence represents the

energy conversion between the eddy perturbation and the mean flow. Furthermore, as EP flux equals zero at the boundary, the energy conversion term can be written as:

$$\begin{aligned}\partial_t \iiint (K' + A') &= -\iiint U(y, z, t) \nabla \square F = -\iiint dydz U \nabla \square F \\ &= -\iiint dydz U \partial_y F_y - \iiint dydz U \partial_z F_z \\ &= \iiint dydz F_y \partial_y U + \iiint dydz F_z \partial_z U\end{aligned}$$

The first term in the right-hand side of equation is the barotropic conversion term, which involves the horizontal shear of the mean flow and horizontal component of EP flux, denoting the conversion between the mean kinetic energy and eddy kinetic energy; the second term is the baroclinic conversion term, which relates to the vertical shear (horizontal density gradient) of the mean flow and the vertical component of the EP flux, denoting the conversion between the mean potential energy and eddy potential energy.

*Supported by NSCF Outstanding Young Scientist Award (Grant No. 40625017) and the National Basic Research Program of China (Grant No. 2006CB403604). The research was also supported by W. Alan Clark Chair from Woods Hole Oceanographic Institution for RXH and NOAA GLERL contribution No. 1462 for JW.*

## Reference

- 1 Gnanadesikan A. A simple predictive model for the structure of the oceanic pycnocline. *Science*, 1999, 283: 2077-2079
- 2 Webb D J, de Cuevas B A. On the fast response of the Southern Ocean to changes in the zonal wind. *Ocean Sci. Discuss.*, 2006, 3: 471-501
- 3 Matthews A J, Meredith M P. Variability of Antarctic circumpolar transport and the Southern Annular Mode associated with the Madden-Julian Oscillation. *Geophys. Res. Lett.*, 2004, 31, L24312, doi: 10.1029/2004GL021666
- 4 Aoki S. Coherent sea level response to the Antarctic Oscillation. *Geophys. Res. Lett.*, 2002, 29(20), doi: 10.1029/2002GL015733
- 5 Hughes C W, Woodworth P L, Meredith M P, Stepanov V, Whitworth T III, Pyne A. Coherence of Antarctic sea levels, Southern Hemisphere Annular Mode, and flow through Drake Passage.

- Geophys. Res. Lett., 2003, 30(9), doi: 10.1029/2003GL017240
- 6 Hughes C W, Meredith M P, Heywood K J. Wind-forced transport fluctuations at Drake Passage: A southern mode. *J. Phys. Oceanogr.*, 1999, 29(8), 1971-1992
  - 7 Meredith M P, Woodworth P L, Hughes C W, Stepanov V. Changes in the ocean transport through Drake Passage during the 1980s and 1990s, forced by changes in the Southern Annular Mode. *Geophys. Res. Lett.*, 2004, 31, L21305, doi: 10.1029/2004GL021169
  - 8 Hughes C W, Stepanov V. Ocean dynamics associated with rapid J2 fluctuations: Importance of circumpolar modes and identification of a coherent Arctic mode. *J. Geophys. Res.*, 2004, 109, C06002, doi: 10.1029/2003JC002176
  - 9 Borowski D, Gerdes R, Olbers D. Thermohaline and wind forcing of a circumpolar channel with blocked geostrophic contours. *J. Phys. Oceanogr.*, 2002, 32: 2520-2540
  - 10 Gnanadesikan A, Hallberg R W. On the relationship of the Circumpolar Current to Southern Hemisphere winds in coarse resolution ocean models. *J. Phys. Oceanogr.*, 2000, 30: 2013-2034
  - 11 Vallis G K. Large-scale circulation and production of stratification: Effects of wind, geometry, and diffusion. *J. Phys. Oceanogr.*, 2000, 30, 933-954
  - 12 Henning C C, Vallis G K. The effects of mesoscale eddies on the stratification and transport of an ocean with a circumpolar channel. *J. Phys. Oceanogr.*, 2005, 35, 880-896
  - 13 Carton J A, Chepurin G, Cao X H, Giese B. A Simple Ocean Data Assimilation analysis of the global upper ocean 1950-95. Part I: Methodology. *J. Phys. Oceanogr.*, 2000, 30: 294-309
  - 14 Hartmann D L, Lo F. Wave-driven zonal flow vacillation in the Southern Hemisphere. *J. Atmos. Sci.*, 1998, 55: 1303-1315
  - 15 Nigam S. On the structure of variability of the observed tropospheric and stratospheric zonal-mean zonal wind. *J. Atmos. Sci.*, 1990, 47: 1799-1813
  - 16 Thompson D W J, Solomon S. Interpretation of recent Southern Hemisphere climate change. *Science*, 2002, 296: 895-899
  - 17 Gillett N P, Thompson D W J. Simulation of recent Southern Hemisphere climate change. *Science*, 2003, 302: 273-275
  - 18 Yang X Y, Huang R X, Wang D. Decadal changes of wind stress over the Southern Ocean associated with Antarctic ozone depletion. *Journal of Climate*, 2007, 20: 3395-3410
  - 19 Fyfe J C, Saenko O A. Human-induced change in the Antarctic Circumpolar Current. *J. Clim.*

- 2005, 18: 3068-3073
- 20 Saenko O A, Fyfe J C, England M H. On the response of the oceanic wind-driven circulation to atmospheric CO<sub>2</sub> increase. *Clim. Dyn.*, 2005, 25: 415-426.
  - 21 Hallberg R, Gnanadesikan A. An exploration of the role of transient eddies in determining the transport of a zonally reentrant current. *J. Phys. Oceanogr.*, 2001, 31: 3312-3330
  - 22 Meredith M P, Hogg A M. Circumpolar response of Southern Ocean eddy activity to a change in the Southern Annular Mode. *Geophys. Res. Lett.*, 2006, 33, L16608, doi: 10.1029/2006GL026499
  - 23 Johnson G C, Bryden H L. On the size of the Antarctic Circumpolar Current. *Deep-Sea Res.*, 1989, 36: 39-53
  - 24 Olbers D, Borowski D, Völker C, Wolff J. The dynamical balance, transport and circulation of the Antarctic Circumpolar Current. *Antarctic Science*, 2004, 16(4): 439-470
  - 25 Zhou T., Yu R. Sea-surface temperature induced variability of the Southern Annular Mode in an atmospheric general circulation model. *Geophysical Research Letters*, 2004, 31, L24206, doi:10.1029/2004GL021473
  - 26 Wang J, Ikeda M. Diagnosing ocean unstable baroclinic waves and meanders using the quasigeostrophic equation and Q-vector method. *J. Phys. Oceanogr.*, 1997, 27: 1158-1172
  - 27 Olbers D, Ivchenko V O. On the meridional circulation and balance of momentum in the Southern Ocean of POP. *Ocean Dynamics*, 2001, 52: 79-93
  - 28 Eliassen A, Palm E. On the transfer of energy in stationary mountain waves. *Geofys. Publ.*, 1961, 22(3): 1-23